

Experiment 6 & 7:
Harmonic Oscillator Part II.
Physical Pendulum. Waves on a Vibrating String.
Denise Wang-

Abstract: 250 words
Body: 2,517 words

Lab performed on: May 29, 2018
Lab section: Lab 6- Tuesday 11am
TA: Narayana Gowda, Shashank
Partners' names:

Harmonic Oscillation of a Physical Pendulum and Waves on a Vibrating String

D. Wang¹

Abstract

In mechanics, a physical pendulum is a rigid body that is able to swing freely about a pivot point. If given an amplitude about its equilibrium point, it undergoes simple harmonic motion. In the first experiment, the oscillations of a physical pendulum were studied in undriven conditions in three regimes of damping. These various damping forces were created by the spaced damping magnets, which gaps that depended on the velocity of the pendulum. At the specific frequency of $f_R = 0.735 \pm 0.001$ Hz, the driving frequency was introduced to the underdamped oscillations and the system oscillated with maximum amplitude. The Q calculated with underdamped oscillations in this part of the experiment equalled 4.1 ± 0.2 , which was calculated using the damping time $\tau = 2.2 \pm 0.1$ s and the angular resonant frequency $\omega_R = 4.467 \pm 0.006$ rad/s.

In the second experiment, the resonance of a oscillating string was observed. The string was stretched and clamped on one end and was attached on the opposite end to the three different masses hanging on the pulley. Three different tensions speeds of the waves were recorded from the photodiode signal plot and were later compared to the initial values, which were calculated based on the linear mass density and tension. Then, the frequencies of various modes were graphically analyzed and compared to the predicted formula frequencies, which was derived from the wave speed $v = 25.9 \pm 0.2$ m/s caused by the 400 g mass. Overall, this allowed for a better understanding of the resonance phenomena for the standing waves.

¹Department of Physics, UCLA

Introduction

In mechanics, a physical pendulum is a rigid body that swings freely about a pivot point and undergoes simple harmonic oscillation at its equilibrium point due to an initial displacement and inertia². An aluminum pendulum shaped like an anchor is used as a physical pendulum for three regimes of damping: damped, undamped, and critically damped oscillation. The purpose of this experiment was to get a better understanding the phenomena of the resonance travelling and standing waves. By observing the resonance on a physical pendulum, we are able to apply the principles of mechanics to the standing waves on the oscillating string with tension.

The oscillating aluminum anchor-shaped physical pendulum with low amplitude presented the undamped oscillation. Then, the three regimes of damping were applied to the undriven pendulum by the damping force caused by magnets with various gaps. The wave generator allowed for the driving of the underdamped physical pendulum. During the oscillations, the pendulum experienced its maximum amplitude at a specific resonant frequency.

The oscillating string with different tensions was analyzed afterwards. The speeds were calculated with the three different tensions in the string, which were created by mass blocks that hung on one end of the pulley. Then, these results were compared with the speeds, analyzed from the Lissajous plots containing photodiode signal vs time. The resonant frequencies of various mode were obtained from the specific speed with the tension calculated earlier in the experiment. These frequencies were compared to the values that were estimated from the Lissajous plots. Last, the harmonic amplitudes were observed when a node was reproduced at the center of the string. Overall, this experiment allowed for more understanding of resonance and harmonic frequencies of the waves.

Methods

The setup for the first experiment consisted of the apparatus as shown in figure 6.11. Furthermore, the photogate, wave driver, damping magnets with the variable spacing, rotation sensor, PASCO 850 Universal Interface, and PASCO Capstone version 1.0.1. The purpose of this was to observe how an aluminum anchor-shaped physical pendulum results in simple harmonic oscillations. The pendulum angular reading was set to zero prior to the start of the experiment. Since friction can lead to an inappropriate damping force and affect how the magnets work, we avoided systematic error by placing the pendulum and magnets at the same level.

The pendulum swung with a small amplitude to ensure that approximations in the calculations were accurate. The damping force was present at all times, since the bottom of the pendulum did not leave the gaps between the magnet. Using photogate for the starting position helped maintain the same initial amplitude. The pendulum swung while the DAQ recorded the angular displacement vs time using the rotation sensor. The set of data without the magnets of the undamped oscillations and five sets of damped oscillations with various gaps of 10, 15, 25, 35, and 45 mm between the magnets were both recorded.

The gaps that undergone critical damping was determined using Scope in the Capstone. This determined which of the gaps allowed the pendulum to come to a stop the fastest. The gap was at a 1mm step for the precision of the data.

The gaps between the magnets were set to be 25mm, and the pendulum was forced to a stop at 8 seconds so that there was no excessive data collected. Then, the Signal Generator produced a sinusoidal driving torque and the driving frequency was set to equal the resonance frequency for undriven undamped oscillations. Then, the resonant frequency was found by

changing the voltage and the graph display of the Lissajous plot. The uncertainty of the frequency was estimated because the change in the shape of the Lissajous plot was not recognized. The set of data to that presented the below, above and at resonance oscillations was recorded. After that, the amplitude of the pendulum oscillations was recorded at 10 different drive frequencies.

For the speed of the travelling wave, the apparatus was set up as shown in figure 7.11. The tension in the string was controlled by the masses from the pulley. The tip was positioned 2mm away from the clamp and slightly touched the string. The wave driver was moved until the waves were vertically transmitted in the plane, which ultimately eliminated systematic uncertainties that could have been recorded in the data. The laser was set up to in a way that it eliminated the top of the string at rest and was directed at the bottom of the light sensor.

The mass of the entire string M_{total} , the length of the entire string L_{total} , and the string from the clamp to the pulley, L were measured. Then, three different masses (100, 200, 400 g) were hung from one end of the pulley to make the tension in the string, the corresponding vertical length of the string, l was measured. For each tension, the light intensity and output voltage were recorded with its time in Capstone.

The setup of the apparatus of the third part of the second experiment was kept the same and the gap from the laser beam and the pulley was repositioned. The largest mass on the pulley was left and the first harmonic frequency was found using the DAQ by recording the amplitude and observing the greatest frequency of that mode. For the 9 consecutive modes, the resonant frequencies were obtained from the Lissajous plots containing the photodiode signal vs driver output.

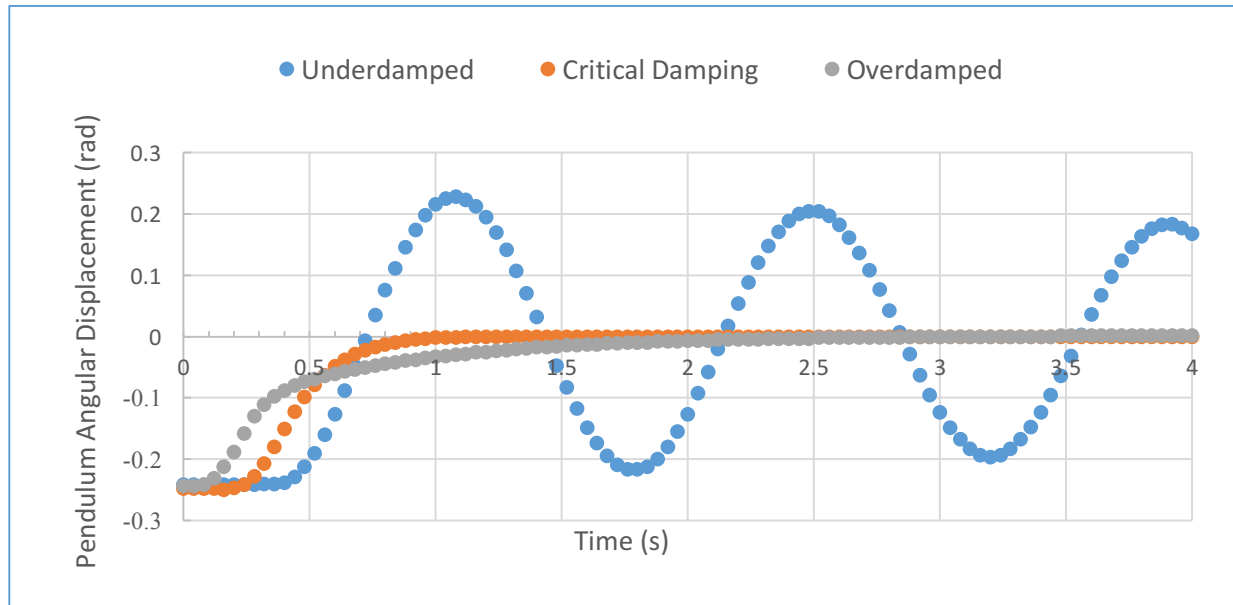
The amplitude of the photodiode oscillations for the second, fourth, and fifth was recorded. The drive amplitude remained unchanged to avoid the systematic error while the movements of the nodes for each harmonic was restricted and the new signal amplitude was recorded. The post was not moved to avoid systematic uncertainties that would have come along with it.

Analysis

The natural angular frequency, ω_0 , was calculated from the data set with undamped undriven oscillations. To find four successive maxima, the data was manually processed and then the average time period, T , was calculated. The formula $\omega = \frac{2\pi}{T}$ was used to calculate the angular frequency: $\omega_0 = 4.86 \pm 0.03 \text{ rad/s}$. The uncertainty was assigned using the expression ii.23¹:

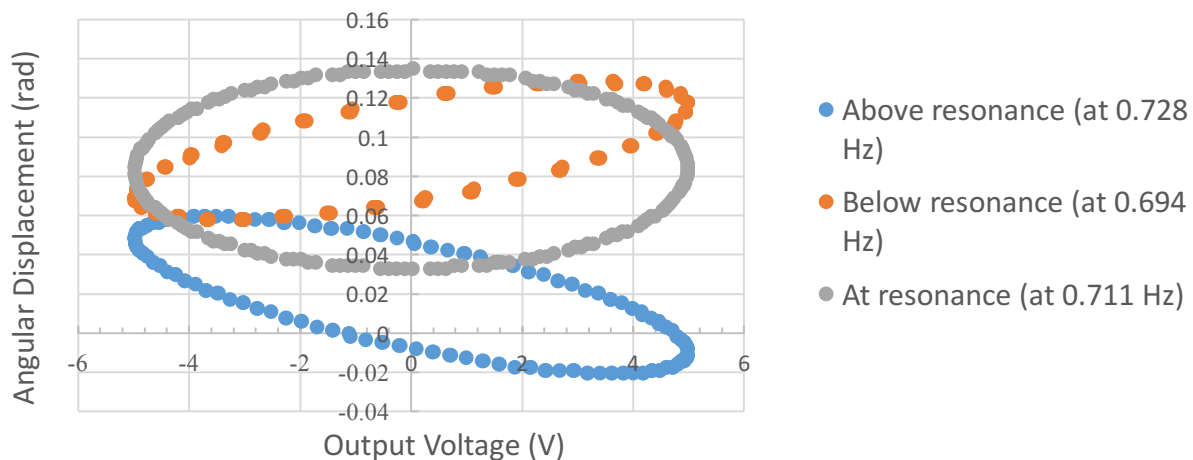
$$\delta\omega_0 = |\omega_0| \frac{\delta T}{|T_{best}|} . \text{ The uncertainty of the time period } \delta T \text{ was calculated by } \frac{T_{max} - T_{min}}{2}$$

Figure 1 – Three Damping Regimes: Overdamped, Underdamped and Critically Damped Oscillations. This plot shows the three regimes of damping, created by the gaps of 10, 24, and 14 mm between magnets with respect to time.



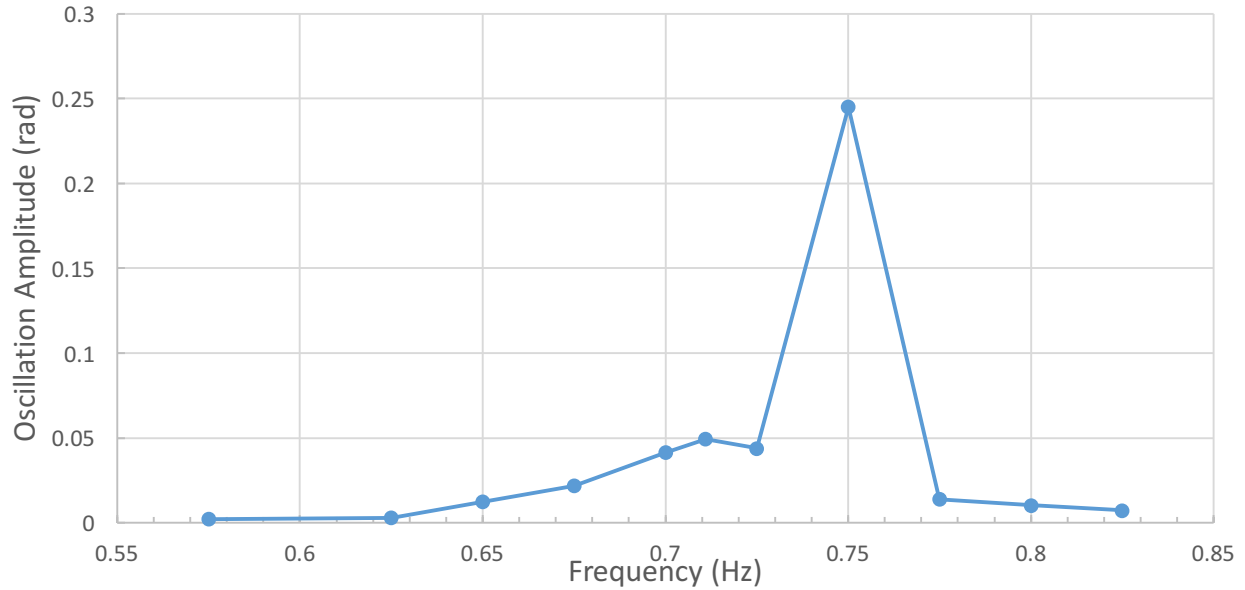
For the resonant angular frequency, the data was recorded for the oscillations with the magnets gaps set at 25mm apart. The shape of the plot presents the underdamped oscillations from Figure 1 with 45mm gaps. The damping time τ was calculated. The time period, $T = 1.61 \pm 0.02$ s, was obtained by measuring the time for three oscillations to occur, 4.82 s, and dividing it by three. The average ratio between four successive maxima was $c = 0.432 \pm 0.006$. The uncertainty was calculated by halving of the time of two successive readings and the uncertainty previously obtained. From the formula 5.13¹, the damping time was calculated to be $\tau = 2.2 \pm 0.1$ s.

Figure 2 – Three Lissajous Plots: Above, Below and At Resonance. These plots show the Lissajous figures for the oscillations of the pendulum with driving frequencies below, above and at resonance. The oscillations at resonance displayed an ellipse that is symmetrical to the y-axis, which presents the output voltage. Therefore, damped oscillator frequency, f_R , is at 0.711 ± 0.001 Hz.



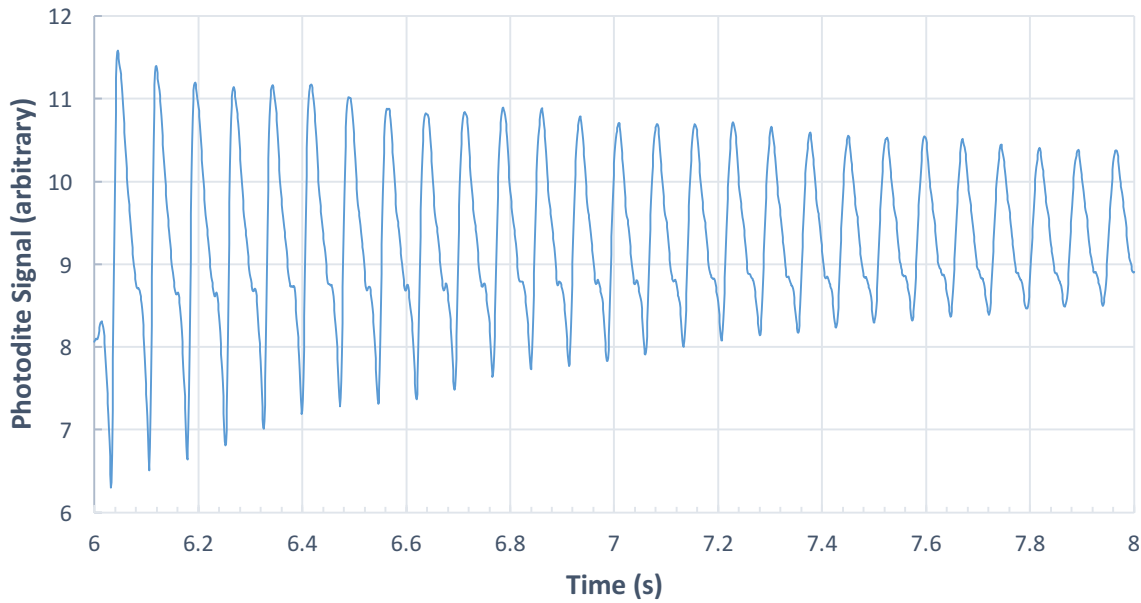
Using $f_R = 0.711 \pm 0.001$ Hz obtained from the Figure 2 the angular frequency ω_R was calculated from $2\pi f_R$, which resulted in 4.467 ± 0.006 rad/s. The uncertainty was derived using expression ii.23¹. By using this value and the damping time, $\tau = 1.6 \pm 0.1$ s, Q was calculated using the equation 6.13 from the Lab Manual¹: $Q = 4.1 \pm 0.2$. The uncertainty in the value of Q was derived from the expression ii.23¹: $\delta Q = |Q_{best}| \sqrt{\left(\frac{\delta\tau}{|\tau_{best}|}\right)^2 + \left(\frac{\delta\omega_R}{|\omega_{R_{best}}|}\right)^2}$.

Figure 3 –Oscillation Amplitude vs Frequency. This plot displays a Lorentzian shape and the maximum oscillation amplitude occurs at the frequency of 0.748 ± 0.001 Hz. The oscillator damped resonance, f_R and the value of Q was estimated from this graph.



Another method other than the graph was used to obtain the value of Q. From Figure 3, the width of the drive frequency was estimated. Then, using formula 6.16¹, the value for Q was calculated to be 4.4 ± 1.6 . Because the graph is not symmetrical, the largest width value was found based on the first symmetry and the smallest width based on the second. The difference was divided by two to get the uncertainty of the width of the drive frequency, $\delta\Delta f = \pm 0.04$ Hz and the value was obtained for $\Delta\omega = 1.3 \pm 0.6$ rad/s. The uncertainty in Q was estimated using the formula $\delta Q = |Q_{best}| \sqrt{\left(\frac{\delta\Delta\omega}{|\Delta\omega_{best}|}\right)^2 + \left(\frac{\delta\omega_0}{|\omega_{0_{best}}|}\right)^2}$, which agreed with the Q obtained from the first method, 4.1 ± 0.2 , since the range from larger Q, 2.6 - 6.2, is within the range of the smaller Q, 4.0 – 4.4. The second method may not be as precise because the graph was not symmetrical which made it difficult to obtain the exact frequencies, which created a large uncertainty. The approximation in the formula 6.16¹ was used and is more accurate for the larger values of Q unlike the small values of Q in this experiment, so the first method can be more trusted for estimating Q.

Figure 4 – Photodiode Signal vs Time of Travelling Wave. The data was collected for three different tensions, 100, 200 and 400g on the pulley. This plot shows the data for the largest mass on the pulley, 400 g. The reoccurring periodic cycles were used to find the average time between cycles Δt and to calculate the wave speeds of each tensions.



From Figure 4, Δt was calculated by finding the time taken for each period features to occur, and dividing by it by one value less. The uncertainty was calculated by dividing the width of the widest periodic point by 2. The wave speed was calculated by dividing the distances travelled between the period cycles by Δt . Another method to find the wave speeds for the three masses was the using formula $M = M_{total} \frac{L_{total}-l}{L_{total}}$ to find the mass of the string from the clamp to pulley. The uncertainty of that value was derived from expressions ii.22 and ii.23¹ $\delta M =$

$|M_{best}| \sqrt{\left(\frac{\delta M_{best}}{|M_{best}|}\right)^2 + \frac{(\delta L_{total})^2 + (\delta l)^2}{(L_{total}-l_{best})^2} + \left(\frac{\delta L_{total}}{L_{total_{best}}}\right)^2}$. The linear mass density μ was calculated by dividing M by L and its uncertainty was calculated from expression ii.23¹ $\delta \mu =$

$|\mu_{best}| \sqrt{\left(\frac{\delta M}{|M_{best}|}\right)^2 + \left(\frac{\delta L}{|L_{best}|}\right)^2}$ and the tension from the mass on the pulley and the hanging mass of the string was found by $T = \left(M_{total} \frac{l}{L_{total}} + m\right) g$. The uncertainty was also derived from expressions ii.22 and ii.23¹ $\delta T =$

$g \sqrt{(\delta m)^2 + \left[\left(\frac{\delta M_{total}}{|M_{total_{best}}|}\right)^2 + \frac{(\delta l)^2}{(l_{best})^2} + \left(\frac{\delta L_{total}}{|L_{total_{best}}|}\right)^2 \right] \left(M_{total} \frac{l}{L_{total}}\right)_{best}^2}$. Finally, the wave speed v was obtained using the formula 7.1¹. The uncertainty was derived from ii.23¹ $\delta v = \frac{|v_{best}|}{2} \sqrt{\left(\frac{\delta T}{|T_{best}|}\right)^2 + \left(\frac{\delta \mu}{|\mu_{best}|}\right)^2}$. All of the uncertainties were calculated based on the formula ii.23¹ provided from the lab manual.

Figure 5 – Measurements of Wave Speeds. This table shows the results of the three different hanging masses obtained from the two methods above.

Hanging Mass on Pulley, m (g) $\pm 0.5\text{g}$	Wave Speed from Figure 4, $v_1(\text{m/s})$	Wave Speed from Formula 7.1 ¹ , $v_2(\text{m/s})$
100	18.6 \pm 2.2	17.4 \pm 0.3
200	21.3 \pm 1.4	20.2 \pm 0.2
400	27.2 \pm 2.6	25.9 \pm 0.2

The values for wave speeds presented in figure 5 agree with each other because the ranges of the values with larger uncertainties are within the ranges of the values with smaller uncertainties. From the wave speed derived from the predicted formula that corresponded with the heaviest mass, $v = 25.9 \pm 0.2/\text{s}$, and the formula 7.3¹, the harmonic frequencies of $n=1, 3, 5, 7$ and 9 were calculated. The uncertainty of these values were also derived from ii.23¹ $\delta f =$

$|f_{best}| \sqrt{(\frac{\delta v}{|v_{best}|})^2 + (\frac{\delta L}{|L_{best}|})^2}$. The resonant frequencies for the modes of first fundamental to the highest mode were found from the Lissajous plots. At the resonant frequency, the standing wave plots were symmetrical.

Figure 6 – Five Resonant Frequencies from $n=1$ to $n=9$. This table shows the five resonant frequencies from $n = 1$ to $n = 9$.

Mode of the Frequency, n	Observed harmonic frequency, $f_{observed}$ (Hz) $\delta f_{observed} = \pm 0.005\text{Hz}$	Predicted harmonic frequency, $f_{predicted}$ (Hz)
1	13.554	13.7 \pm 0.1
3	27.005	28.2 \pm 0.4
5	40.515	42.6 \pm 0.6
7	53.946	53.2 \pm 0.7
9	67.623	68.3 \pm 1.3

Figure 6 contains the values calculated by the prediction formula 7.3¹ in the lab manual and the estimated values from the Lissajous plots. Both values match because the ranges created by uncertainties are within each other. As for the 30th mode frequency, it was not obtained during the lab.

Conclusion

The purpose of the experiment was to get a better understanding of the resonance of the standing waves. Harmonic oscillation, the undriven periodic motion of a physical pendulum, was observed under three damping regimes: underdamped, overdamped, and critically damped. The resonance frequency was calculated for driven underdamped oscillations. For the physical pendulum, the value Q was calculated to be 4.1 ± 0.2 , which was obtained from the damping

time $\tau = 2.2 \pm 0.1$ s and the angular driving frequency $\omega_R = 4.467 \pm 0.006$ rad/s. Q was calculated to be 4.4 ± 1.6 , from the width of resonance curve $\Delta\omega = 1.3 \pm 0.6$ rad/s and resonant frequency $\omega_0 = 4.86 \pm 0.03$ rad/s. In comparing the two values of Q together, both values agreed with one another, but the second method was not as precise because the graph was not symmetrical, which overall created a large uncertainty. The speed waves for the string with three different tensions of 100, 200 and 400 g also matched when calculated by two different methods. The calculations of the first method were analyzed from the photodiode signal vs time plot, while the second method was calculated from the formula with the value of tension and the linear mass density that corresponded to each of the different masses. The resonant frequencies of standing waves were also derived from two methods. The calculation of the first method was analyzed from Lissajous plots and the calculation of the second method was analyzed from the values of the speed corresponding with the mass of 400g on the pulley $v = 25.9 \pm 0.2$ m/s as well as the $L = 0.94$ m, which was the length of string between the clamp and pulley. The resonant frequencies had the first fundamental harmonic node $f(1) = 13.554 \pm 0.005$ Hz. This allowed for a prediction the 30th harmonic, which was not obtained experimentally.

A potential source of systematic uncertainty dealt with the beam and the light detector that measured the wave speeds and some signal amplitudes. The light was still accounted for and produced background noise, despite the positioning of the laser, so a systematic error occurred and the readings were ultimately less accurate. This can be avoided next time by using the photogate to monitor the motion of a specific part of the string instead of a photodiode signal graph, which would allow more accurate result rather than smaller and less accurate amplitudes.

References

1. Campbell, W. C. et al. Physics 4AL: Mechanics Lab Manual (ver. August 31, 2017). (Univ. California Los Angeles, Los Angeles, California).
2. Young, H. D., Freedman, R. A. & Ford, A. L. *Sears and Zemansky's University Physics with Modern Physics*. 451 (Pearson, 2015).